Supramolecular Comb Polymers featuring aromatic urea receptor pendant units – the effect of aromatic substitution on material properties

Polymer 337 (2025) 128993

Contents lists available at ScienceDirect

Polymer

journal homepage: www.elsevier.com/locate/polymer

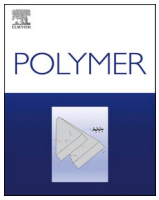

Supramolecular comb polymers featuring aromatic urea receptor pendant units – the effect of aromatic substitution on material properties

Matthew Hyder [a], Claudia Duval [a], Lochlan J. McGregor [a], Alarqam Z. Tareq [a,b], Adam D. O'Donnell [a], Ann M. Chippindale [a], Josephine L. Harries [c], Wayne Hayes [a,*]

[a] Department of Chemistry, University of Reading, Whiteknights, Reading, RG6 6DX, UK
[b] Department of Chemistry, Faculty of Science, University of Zakho, Duhok, 42001, Iraq
[c] Domino UK Ltd, Trafalgar Way, Bar Hill, Cambridge, CB23 8TU, UK

ARTICLE INFO

Keywords:
Supramolecular material
Healable
Nitro substitution
Urea receptors
Comb-polymers

ABSTRACT

Molecular recognition units incorporated in polymer networks can provide a useful avenue for the introduction of dynamic stimuli-responsive properties into bulk materials to permit recovery post-damage. In this study, *meta*- and *para*-nitro substitution on pendant urea groups of polymethacrylate comb polymers has been investigated to establish their effect on the bulk-material properties. The effect of supramolecular interactions on bulk properties was assessed through the creation of a series of comb polymers featuring increasing molar ratios of methacrylate monomers that possess urea recognition units, namely 2-(3-(4-(3-(3-nitrophenyl)ureido)phenyl)ureido)ethyl methacrylate (the *meta* system) or 2-(3-(4-(3-(4-nitrophenyl)ureido)phenyl)ureido)ethyl methacrylate (the corresponding *para* system) with lauryl methacrylate employed as the comonomer. These monomers are capable of forming multiple supramolecular interactions through hydrogen bonding involving the urea and nitro sites. Varying the ratio of supramolecular monomers yielded materials with increased phase separation, mechanical durability, adhesive shear strength, and improved property recovery. The materials that incorporated the *para*-substituted urea recognition unit exhibited enhanced mechanical properties when compared to the *meta* counterparts. The degree of property recovery proved to be comparable across both set of materials: as the supramolecular monomer content was increased in both series, a higher percent of property recovery post-damage was observed.

1. Introduction

The implementation of supramolecular systems in materials can be exploited to incorporate or enhance favourable properties [1,2] in a wide range of common and specialist applications, such as in touchscreens, electrical cables, and bio-medical devices [2,3]. Supramolecular materials utilise secondary interactions such as π-π stacking [4–6], metal-ligand coordination [7,8], host-guest interactions [9,10], and hydrogen bonding [10–13] to form materials capable of self-assembly. When compared to covalent-bonded networks, supramolecular systems can dissociate and reassociate readily when exposed to appropriate external stimuli, such as pH [14], light [15], heat [16], pressure [17,18], magnetic fields [19], or moisture [20]. Stimuli-responsive behaviour can be used to recover physical properties by reforming interactions, which is particularly interesting when achievable under relatively mild or ambient conditions [16,21,22]. Supramolecular interactions within polymeric materials have also been used to introduce commercially attractive properties, such as tuneable adhesion [17,22], and 3D printing [23].

The directional self-assembly [24,25] of non-covalent interactions such as hydrogen bonding [26–28] has been exploited in the design of supramolecular polymer systems. The quadruple hydrogen bonding 2-ureido-4[1H]-pyrimidone (UPy) unit reported by Meijer and co-workers is an excellent example of an efficient self-associating receptor (dimerization constant (K_{dim}) > 10^6 M^{-1}) that permits access to a wide range of stable supramolecular polymers [11,28]. Aromatic π-π

This article is part of a special issue entitled: Bond Breaking in Polymers published in Polymer.

* Corresponding author.
E-mail addresses: m.hyder@pgr.reading.ac.uk (M. Hyder), claudia.duval@pgr.reading.ac.uk (C. Duval), l.mcgregor@pgr.reading.ac.uk (L.J. McGregor), a.z.tareq@pgr.reading.ac.uk (A.Z. Tareq), a.odonnell@protonmail.com (A.D. O'Donnell), a.m.chippindale@reading.ac.uk (A.M. Chippindale), josie.harries@domino-uk.com (J.L. Harries), w.c.hayes@reading.ac.uk (W. Hayes).

https://doi.org/10.1016/j.polymer.2025.128993
Received 8 July 2025; Received in revised form 26 August 2025; Accepted 28 August 2025
Available online 28 August 2025

stacking was employed in a self-complementary pyrene-aromatic diimide tweezer system developed by Colquhoun and co-workers [29] which assembled in solution to form a molecular "Roman Handshake" with a substantial self-association constant (*ca.* 10^5 M^{-1}).

The architecture of a polymer significantly affects the properties in the bulk. Comb-type polymers possess enhanced concentrations of interaction sites when compared to conventional telechelic architectures, a key advantage when designing supramolecular polymer systems [26]. The applications of comb architectures in supramolecular materials include debond-on-demand adhesives [25], polymer coatings [28], and self-healing polymers [30,31]. Comb-polymers utilising hydrogen bonding have been extensively studied [32–34], especially those featuring urea groups [32,34]. The hydrogen-bonding recognition of complementary nucleobase pairs was exploited by Long and co-workers in supramolecular comb polymer blends [31,33,34], which showed enhanced thermomechanical properties, increased shear strength, and dramatic increases in viscosity when compared to the parent polymer backbone.

Structural isomerisation of the receptor sites has also been studied in order to change the physical and mechanical properties of supramolecular systems [15,26,35–38], such as imparting stimuli-responsive behaviour through triggering changes in structural isomerisation [39,40]. This technique was used in a photo-responsive polymeric hydrogel system studied by Stoddart and co-workers [41] whereby *cis/-trans*-isomerism was used to form a highly reversible sol-gel system capable of response under mild conditions. Studies reported by Rodriguez-Llansola et al. [35] and Wood et al. [14] described pH-responsive bisaromatic urea hydrogelators in which the isomers of nitro-substituted aromatic rings were shown to decrease the critical gelation concentration of their materials dependant on substitution (*ortho* > *meta* > *para*). Subsequent studies by O'Donnell et al. [24] introduced *ortho*-methyl groups to the urea framework to promote stronger hydrogen bonding interactions.

The present work has investigated the effect *meta/para*-isomerisation has on pendant bisaromatic urea nitro recognition units using novel supramolecular monomers. The effect of molar loading of these isomeric monomers in a series of supramolecular methacrylate-based comb polymers (SCPs) with respect to their physical, mechanical, self-healing, and adhesive characteristics was established. The copolymerisation of lauryl methacrylate with novel supramolecular monomers enabled the formation of thermally stable films at room temperature with self-healing and adhesive properties.

2. Results and discussion

2.1. Monomer synthesis

The aim of this study was the synthesis and comparison of two series of supramolecular comb polymers (SCPs) with increasing incorporation of a monomer capable of non-covalent interactions, namely hydrogen bonding. The monomer species were designed with multiple hydrogen bonding sites (nitro and urea moieties) which allow for supramolecular interactions [42–47]. The synthetic routes for both the *meta*- and *para*-nitro derivatives followed the general procedure outlined in Scheme 1. Di-*tert*-butyl dicarbonate was used to mono-protect 1,4-phenylenediamine to afford (**1**) in a yield of 94 %. The protected aniline **1** was then reacted with either *m*-nitrophenyl isocyanate or *p*-nitrophenyl isocyanate to give either the *meta* (**2**) or *para* (**3**) bisaromatic urea, after which deprotection using conc. HCl afforded the aniline bisaromatic ureas, **4** and **5**. The aniline moieties of **4** or **5** were then reacted with 2-isocyanatoethyl methacrylate to yield the desired *meta*- or *para*--monomers (**6**) and (**7**), respectively. The synthetic protocols used to generate these compounds and the associated characterisation data for the synthesised materials can be found in the supporting information (SI) file (see Figs. S1–S14).

Single crystals of the bisaromatic urea monomers **6** and **7** were grown via slow evaporation, the solid-state structures reveal hydrogen bonding through the urea and carbonyl groups (see SI Figures S15-S18 plus Tables S1–S7 for the solid-state structures and data). The *para*-substituted bisaromatic urea monomer, **7**, co-crystallised with DMF and reveals hydrogen bonding through the carbonyl of the methacrylate group implying that the *para* monomer may form less ordered assemblies than the monomer bearing the *meta* substituent. This hypothesis is supported by data from the literature for analogous *meta*-substituted nitroaromatic ureas which exhibit well-defined crystalline structures [13,48]. The co-crystallisation of **7** with DMF hinders the direct comparison between the two monomers, however, there are some noteworthy points that relate to bulk properties of the polymers featuring this monomer. The electron withdrawing effect of the *meta*-nitro group in **6** is evident in the shortening of the urethane hydrogen bonds on adjacent molecules.

2.2. Synthesis of comb-polymers

To generate the supramolecular comb-polymers, bisaromatic urea monomers **6** (*meta*) and **7** (*para*) were copolymerised with lauryl methacrylate via free-radical polymerisation using azobisisobutyronitrile (AIBN) as the initiator, see Scheme 2. The molar feed ratios of **6** and **7** were varied between 2.5 % and 12.5 % to afford five SCPs for each series, together with poly(lauryl methacrylate) (**PLMA**) homopolymer as a baseline for comparison. The compositions of the SCPs are detailed in Table 1. The synthetic procedures used to generate **SCP1**-**SCP10** and **PLMA** and associated characterisation data can be found in the SI file (see Figs. S19–51).

The synthesis of **SCP1**-**SCP10**, as well as polylauryl methacrylate (PLMA) was confirmed via NMR and IR spectroscopy, and GPC analysis (see Table 1 and Figs. S19–51). ^{1}H NMR spectroscopic analysis confirmed that the polymer compositions matched their corresponding

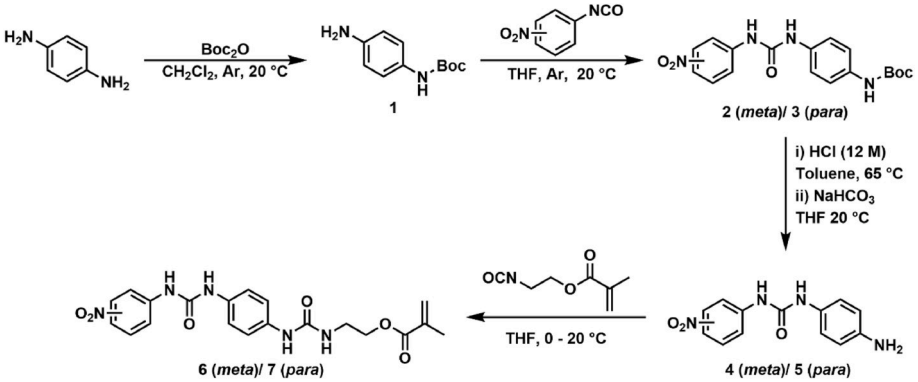

Scheme 1. Synthesis of the methacrylate supramolecular monomers **6** and **7**.

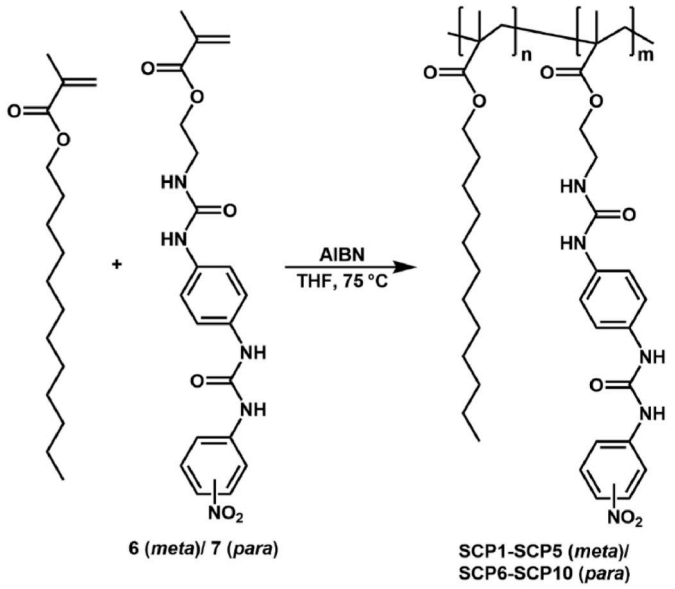

Scheme 2. Synthesis of **SCP1**-**SCP10** using lauryl methacrylate and bisaromatic urea monomers **6** and **7**.

Table 1
Composition and GPC data for **PLMA** and **SCP1**-**SCP10**.

Polymer	*meta* (6)/*para* (7)	mol% of 6/7	M_n (g mol^{-1})	M_w (g mol^{-1})	Đ
PLMA	–	0.0	43000	137000	3.19
SCP1	**6**	2.5	71000	451000	6.35
SCP2	**6**	5.0	179000	1480000	8.27
SCP3	**6**	7.5	82000	978000	11.93
SCP4	**6**	10.0	140000	1416000	10.11
SCP5	**6**	12.5	130000	1257000	9.67
SCP6	**7**	2.5	117000	791000	6.76
SCP7	**7**	5.0	281000	1550000	5.52
SCP8	**7**	7.5	390000	1890000	4.85
SCP9	**7**	10.0	441000	3576000	8.11
SCP10	**7**	12.5	981000	3329000	3.39

feed ratios of monomers. The molecular weights of the SCPs were assessed via GPC analysis and the polymers showed significant increases in the M_n, M_w, and dispersity (Đ) as the mol% of the supramolecular monomers **6** and **7** was increased, see Table 1. This trend likely occurred as a result of the self-association of the polymer chains yielding aggregates under the analytical conditions employed [49]. Variable-temperature infrared (VT-IR) spectroscopic analysis was performed on **SCP4** (meta) and **SCP9** (para) via heating-cooling cycles ranging from 25 °C to 150 °C and then back to 25 °C. The deconvolution of the urea carbonyl groups were monitored as a function of temperature, see Fig. S52. All polymers observed shifting of the urea carbonyl and N–H bending vibration with increasing temperature, indicating dissociated hydrogen bonding network [48,50].

2.3. Thermal analysis

Thermogravimetric analysis (TGA) was conducted from 20 to 550 °C under nitrogen at a heating rate of 10 °C min^{-1} to determine the maximum processing temperature of the polymers. All of the SCPs exhibited greater thermal stability and higher onsets of degradation when compared to **PLMA**, with complete degradation of all polymers evident at 450 °C (Table 2, Figures S53-S63).

To determine thermal transitions of the SCPs, differential scanning calorimetry (DSC) was utilised from −80 to 150 °C at a heating and cooling rate of 5 °C min^{-1} (Table 2, Figures S64-S74). The amorphous

Table 2
Thermal analysis of **PLMA** and **SCP1**-**SCP10**.

Polymer	*meta* (6)/*para* (7)	mol% of 6/7	Onset of degradation (°C)	T_g (°C)[a]
PLMA	–	0.0	255.46	−54.06
SCP1	**6**	2.5	267.95	−50.33
SCP2	**6**	5.0	278.45	−49.68
SCP3	**6**	7.5	271.59	−49.19
SCP4	**6**	10.0	269.17	−48.61
SCP5	**6**	12.5	276.83	−47.26
SCP6	**7**	2.5	268.76	−51.19
SCP7	**7**	5.0	274.10	−50.39
SCP8	**7**	7.5	274.10	−49.85
SCP9	**7**	10.0	268.77	−49.32
SCP10	**7**	12.5	257.15	−48.03

[a] Second heating run at 5 °C min^{-1}.

nature of all the SCPs was revealed by the singular observation of a glass transition (T_g) for each polymer, the lack of other features implying that no long-range ordering was present within the systems. **PLMA** exhibited a T_g at −54.06 °C, consistent with literature values [46]. The polymers containing monomers **6** (*meta*) or **7** (*para*) exhibit a rise in T_g as the loading of the supramolecular monomers increased: from −50.33 to −47.26 °C in the *meta*-substituted series; from −51.19 to −48.03 °C in the *para*-substituted series. These shifts were attributed to hydrogen bonding within the SCP networks. This phenomenon has also been observed by Long and co-workers [51] and Shi et al. [46], but the shift in the T_g values of the SCPs in this study was smaller than observed for UPy and amide functionalised comb polymer systems. The scale of the shift in T_g values was attributed to the broad polydispersity of these SCPs. The series (**SCP1**-**SCP5**) bearing the *meta*-receptors exhibited a higher T_g at every mol% loading than the corresponding *para*-SCP, indicating increased ordering within the amorphous matrix.

2.4. Atomic force microscopic analysis

Microphase separation of the SCPs was revealed by atomic force microscopy (AFM). The topographical AFM images are shown in Fig. 1 and Figures S75-S77 for **SCP3**-**SCP5** and **SCP8**-**SCP10**, respectively. AFM analysis of each polymer revealed two distinct aspects: the hard domains, evident as dark areas, are present on account of the low phase-angle shift; the bright regions were attributed to the soft domains, because of the high phase-angle shift [46,53–57]. AFM analysis of **PLMA**, **SCP1**, **SCP2**, **SCP6**, and **SCP7** was not conducted based on the viscous nature of the polymers at ambient conditions.

Uneven surface morphologies were observed in both phase- and height-tapping analysis modes corresponding to phase separation in **SCP3**-**SCP5**. The changes in hard domains across both SCP series were attributed to increasing hydrogen bonding interactions of the pendant bisaromatic urea units, whereas the soft domains were attributed to van der Waals' forces, primarily from the lauryl methacrylate sections of the polymers. The hard domains were observed as isolated spherical and cylindrical features with dimensions of *ca*. 128–133 nm (**SCP3**) and *ca*. 129–135 nm (**SCP4**), consistent with AFM data of structurally-related materials [51–57]. The observed features in AFM images the AFM images can be attributed to supramolecular association of the hydrogen bonding monomers during the polymerisation that lead to formation of clusters of blocks in the polymer backbone in the solid state. These features merged and formed well-defined assemblies, evident as highly branched (>3 branches) 'wormlike' aggregates. These dense nanodomains imply a high level of mechanical contrast between the hard and soft domains [48]. Bouteiller and co-workers [58] also observed this dramatic development in phase separation phenomena; they suggested that significant differences in the morphology of the polymers were observed as a result to the self-assembling between the polymer chains via hydrogen bonding units (functionality of the polymer), which might enhance the phase separation. These findings reveal the possibility to

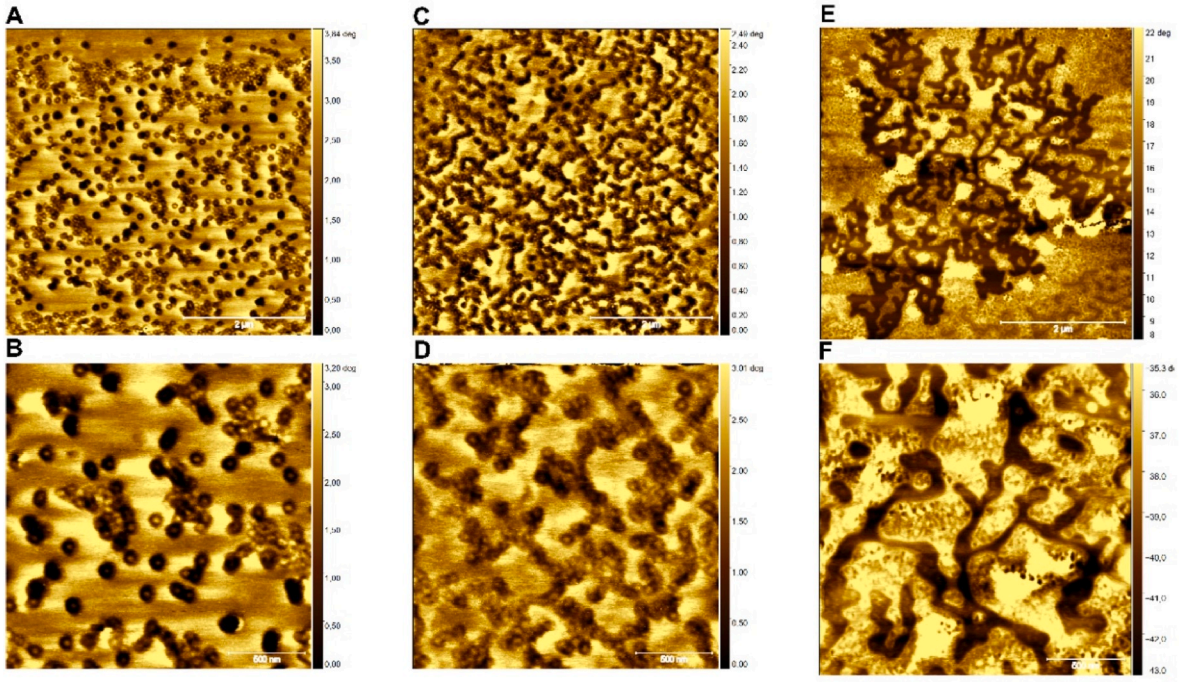

Fig. 1. AFM tapping mode phase images of **SCP3** (**A** and **B**), **SCP4** (**C** and **D**), and **SCP5** (**E** and **F**); the scale bars = 2 μm and 500 nm. All the SCP polymer samples were prepared by drop casting from THF (0.5 mg mL^{-1}) on freshly cleaved mica discs.

tune polymer-decorated supramolecular morphology with increasing of the monomer loading. In the case of **SCP5**, the dimensions of the phase-separated regions were found to be *ca.* 60–80 nm wide but extended in length (800–900 nm), as a result of the high density of hydrogen-bonding interactions provided by the increased monomer loading (12.5 mol%). Evenly distributed hard domains with dimensions

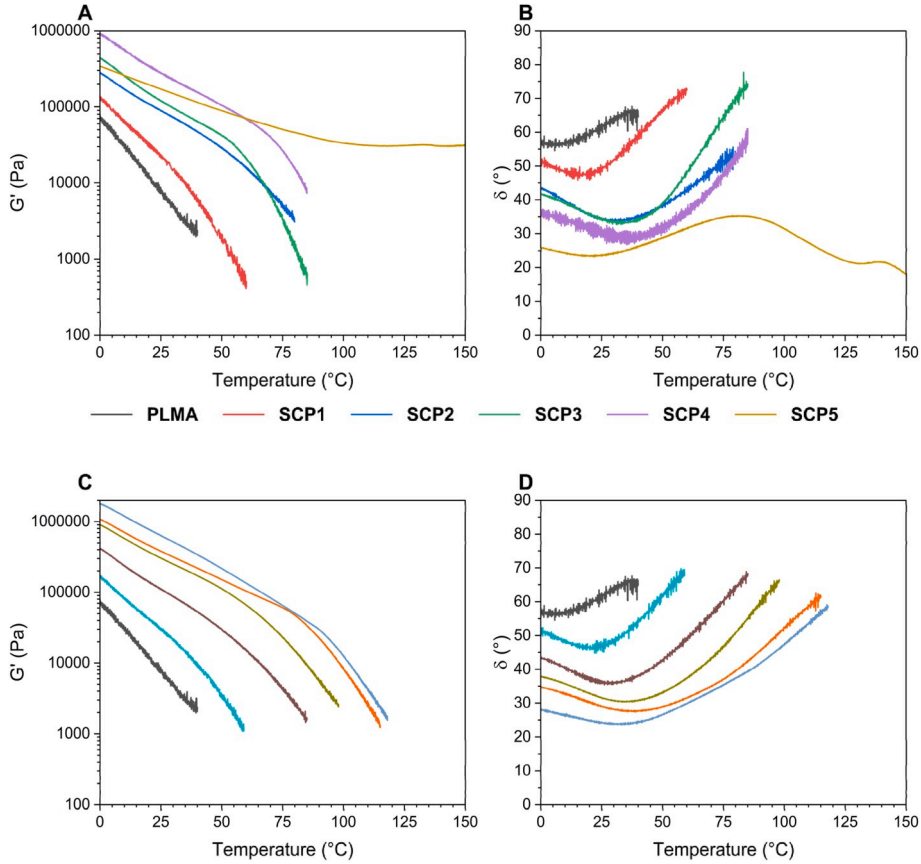

Fig. 2. Storage modulus *vs.* temperature plot (**A**) and phase angle *vs.* temperature plot (**B**) of **SCP1-SCP5**, and analogous plots (**C**) and (**D**) for **SCP6-SCP10**.

ca. 50–70 nm were observed for **SCP8** (see Figures S76 A, B and S77 A, B), attributed to aggregation via hydrogen bonding between polymer chains [51,53]. The phase images of **SCP8** and **SCP9** revealed the aggregation of hard segments, from small well-percolated microphase separated areas in **SCP8**, to larger aggregated regions in **SCP9** [53]. **SCP10** exhibited different features when compared to **SCP8** and **SCP9**, as well as those displayed by **SCP5**, i.e. less branched in nature with dimensions *ca.* 1–2 μm. The phase-separated morphology of **SCP10** derived from the highly ordered hard domains aggregating with strong hydrogen-bonding associations between the polymer chains from the *para*-nitro bis aromatic urea unit**,** see Figures S76 (E, F) and S77 (E, F).

2.5. Rheological analysis

Investigation of the viscoelastic properties of the SCPs was conducted through dynamic rheological testing over a temperature range of 0–150 °C, see Fig. 2, Table 3. Figures S78 and S79 also show the corresponding G" (viscous behaviour) of the polymers – the viscoelastic transition for these materials is evident at 45° in Fig. 2B and D. Increasing storage modulus (G') values over the series reveals stronger interactions in the materials, as more energy is absorbed and flow is resisted. There is some discrepancy in the trend over the *meta* series, as **SCP2** (5.0 mol%) exhibits more elastic behaviour than expected at higher temperatures, whereas **SCP3** (7.5 mol%) showed lower than expected elastic behaviour. This was reflected in both the crossover temperatures and the storage moduli. Across the series, the *meta* series generally exhibited lower storage moduli than their *para*-series. This trend is in agreement with the variations in the phase separation between the *meta* and *para* series as evident from the AFM analysis.

Rheological analysis in Table 3 shows that increasing the mol% of the bisaromatic urea monomers **7**/**8** in the comb polymers causes the resulting polymer material to exhibit more elastic behaviour, a trend in agreement with previous studies [34,46].

2.6. Tensile analysis

The effects of the regio-isomerisation and loading of the supramolecular monomers have on the mechanical properties of the SCPs was investigated through the use of stress-strain tensile tests at a rate of 10 mm min^{-1} (see Fig. 3). The viscous nature of the SCPs with lower content of the bisaromatic urea pendant units (5.0 % and under, i.e. **SCP1**, **SCP2**, **SCP6**, and **SCP7**) excluded them from assessment of the tensile properties as self-supporting films could not be formed.

The ultimate tensile strength (UTS) and the Young's modulus (YM) of the materials reveal a steady increase with molar ratios for both the *meta* and *para* series, with the exception of **SCP5** (see Table 4). The results of **SCP5** could be attributed to high degrees of interchain association and subsequent nanoparticulate formation, because of the high mol% loadings of the strongly supramolecular associating monomer **6**. Exact break points were difficult to attain as a consequence of the viscoelastic nature of the materials, leading them to slowly tear rather than producing clean breaks. However, it was possible to observe that, as the mol% of the supramolecular monomer was increased, the strain at break decreased. This trend is consistent with the data reported for analogous supramolecular comb polymers [46], i.e. increasing the loading of supramolecular bonding sites affords enhancements in material properties. There is a clear distinction between the mechanical properties of the *meta* and *para* series, where the *para*-SCPs outperform their *meta* counterparts for all mol% loadings. An analogous trend has been observed for end-capped telechelic polyurethanes, whereby the 4-nitroaniline end-capped SPU exhibited higher UTS and YM values when compared to its *meta*-substituted counterpart [49].

Table 3
Rheological analysis of **PLMA** and **SCP1-SCP10**.

Polymer	*meta* (6)/*para* (7)	mol% of 6/7	G' at 25 °C (Pa)	Crossover temperature (°C)
PLMA	–	0.0	7200	N/A
SCP1	**6**	2.5	23600	N/A
SCP2	**6**	5.0	88200	63.8
SCP3	**6**	7.5	118800	57.3
SCP4	**6**	10.0	273800	71.5
SCP5	**6**	12.5	171500	N/A
SCP6	**7**	2.5	31000	N/A
SCP7	**7**	5.0	109500	53.9
SCP8	**7**	7.5	305200	72.5
SCP9	**7**	10.0	380600	89.3
SCP10	**7**	12.5	633800	95.9

2.7. Adhesion studies

The SCPs capable of forming stable films at ambient temperatures (**SCP3-SCP5** and **SCP8-SCP10**) were investigated for their use as hot-melt adhesives and ability to undergo multiple re-adhesion cycles on glass and aluminium substrates (Fig. 4 and Tables S8 and S9). Materials featuring urea hydrogen bonding systems have had their adhesive properties studied extensively by Bouteiller et al., as well as how supramolecular structuring changes these properties [59,60]. The *meta*--nitro functionalised SCPs (**SCP3-SCP5**) exhibited shear strengths *ca.* 0.5–0.6 MPa, with only marginal increases in shear strength as the content of the supramolecular monomer was increased. In contrast, the *para*-nitro functionalised SCPs (**SCP8-SCP10**) revealed significant increases in shear strength when increasing the mol% incorporation of the bisaromatic urea monomer **7**. An increase of 5.0 mol% loading (i.e. 7.5 mol% in **SCP8** to 12.5 mol% in **SCP10**) resulted in an increase of over 450 % in shear-strength on both glass and aluminium. These increases were attributed to the dissociation of the weaker and less ordered hydrogen-bonding networks within the *para*-nitro polymers, allowing the formation of hydrogen-bonding interactions with, and increased wetting of, the surface of the glass and substrates [61]. This result is in agreement with a previous study investigating end-group and steric effects, which demonstrated that when *para*-nitro substitution was present, adhesion to both glass and aluminium increased 1.34 MPa and 1.36 MPa, respectively, when compared to the *meta*-nitro system [45].

This trend was attributed to an interruption of the ordering caused by the substitution pattern of the hydrogen-bond receptor. However, when increasing the mol% content of **7** in the *para*-nitro series, reduction in shear-strength of up to 58 % upon the first re-adhesion was observed, and this value was maintained over subsequent re-adhesion cycles. This decrease was attributed to the thermal processing that the SCPs were subject to, potentially causing destabilisation of the ordered supramolecular networks.

2.8. Self-healing studies

Visualisation of the self-healing process in real-time was achieved using variable-temperature optical microscopy (Figures S81-S84). The SCPs were cut into two pieces, then placed in contact on the hot-stage microscope stage, where the sample was heated from 20 °C at a rate of 10 °C min^{-1}. Adjusting the non-covalent crosslinking density of the SCPs through increases in the supramolecular monomer (**6**/**7**) loadings led to shifts in the temperature required for onset and completion of healing to higher temperatures. The influence of the substitution pattern of the nitroaromatic unit on the observed healing is consistent with the rheological data shown in section 2.5, with the *para*-SCPs (**SCP9** and **SCP10**) showing complete healing at 120 °C, indicative of their crossover temperatures. Of the *meta*-SCPs (**SCP4** and **SCP5**), however, only **SCP4** was found to have a crossover temperature within 0–150 °C, **SCP5** did not exhibit a transition into viscous behaviour, supported by the incomplete healing of the sample because of the lack of material flow.

Healing efficiency was investigated through tensile testing post-damage. Once suitable healing temperatures were found via thermal testing, the materials were healed at *ca.* 10 °C below their viscoelastic

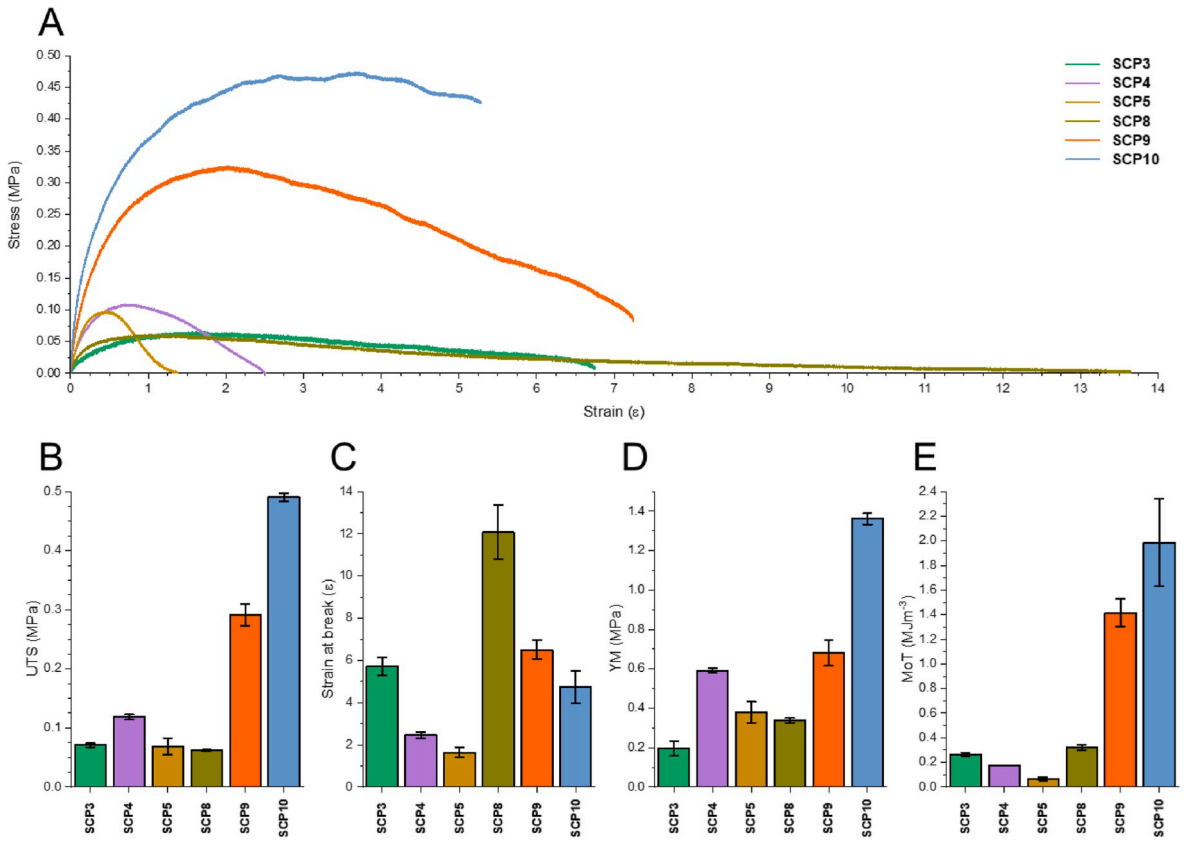

Fig. 3. (**A**) Representative stress-strain curves of **SCP3**-**SCP5** and **SCP8**-**SCP10**. Comparison of (**B**) ultimate tensile strength (UTS), (**C**) strain at break, (**D**) Young's Modulus (YM), and (**E**) Modulus of Toughness (MoT). The error shown is the standard deviation for the three repeats of each sample.

Table 4
The effect of *meta*-/*para*-nitro isomerisation of the recognition motif on the mechanical properties of the SCPs. The values recorded are the averages of three separate samples for each CEPU. The error shown is the standard deviation for the three repeats of each sample.

SCP	*meta* (6)/*para* (7)	mol% of 6/7	UTS (MPa)	Strain at break (ε)	Young's Modulus (MPa)	Modulus of Toughness (MJ m^{-3})
SCP3	**6**	7.5	0.07 ± 0.00	5.73 ± 0.4	0.20 ± 0.4	0.26 ± 0.01
SCP4	**6**	10.0	0.12 ± 0.00	2.47 ± 0.2	0.59 ± 0.01	0.18 ± 0.00
SCP5	**6**	12.5	0.07 ± 0.01	1.63 ± 0.2	0.38 ± 0.05	0.07 ± 0.01
SCP8	**7**	7.5	0.06 ± 0.01	12.07 ± 1.3	0.34 ± 0.01	0.32 ± 0.02
SCP9	**7**	10.0	0.29 ± 0.02	6.50 ± 0.4	0.68 ± 0.1	1.41 ± 0.1
SCP10	**7**	12.5	0.49 ± 0.01	4.73 ± 0.8	1.36 ± 0.03	1.99 ± 0.4

transition (determined via rheological analysis) for 3 h, with cut pieces placed in contact. This allowed for the dissociation and re-association of supramolecular interactions and suitable material flow. The polymers were then cooled under ambient conditions to room temperature before tensile tests were performed (Table 5). Healing efficiencies were derived by calculating the percentage of individual property values recovered after damage. Several properties recovered beyond their pristine values, a common phenomenon for supramolecular polymers, attributed as a consequence of the supramolecular networks within the prepared pristine/healed material having not attained their thermodynamic minimum [62]. The healing studies show that SCPs featuring *meta* nitro groups generally recover their properties to a larger extent than their *para* counterparts, with exceptions seen in **SCP9** UTS and YM, and **SCP10** strain at break. This outcome was rationalised by consideration of the studies reported by Neumann et al. who investigated the effect of the rate of entanglement in the context of healable materials. The study concluded that less mobile macromolecules, such as the larger polymers featuring the *para* substituted monomer, require more time for healing than more mobile macromolecules [63].

3. Conclusions

This paper reports the successful synthesis of two series of supramolecular comb-polymers (SCPs) with different mol% loadings of bisaromatic urea monomers which feature either *meta*- or *para*--nitro pendant groups. Analysis of the polymer series show that increasing incorporation of supramolecular units increases thermal and rheological properties of the bulk materials, leading the polymers to transition from viscous liquids to viscoelastic solids at ambient conditions. The regioisomeric differences imparted by the *meta*/*para*-nitro recognition moieties became evident within the mechanical analysis of the SCPs, where the *para*-nitro SCPs exhibited increased UTS and elongation at break relative to their *meta* counterparts, despite crystallographic analysis of the monomer suggesting less ordered assemblies. The adhesive properties of the SCPs showed re-adhesion to glass and aluminium substrates could be achieved without loss of shear strength over three re-adhesion cycles and initial shear strength up to 3.93 MPa could be achieved. The SCPs were also found to exhibit self-healing behaviour upon exposure to thermal stimuli, with modest recoveries of the mechanical properties observed. Ultimately this study highlights how *meta*/*para*-nitro

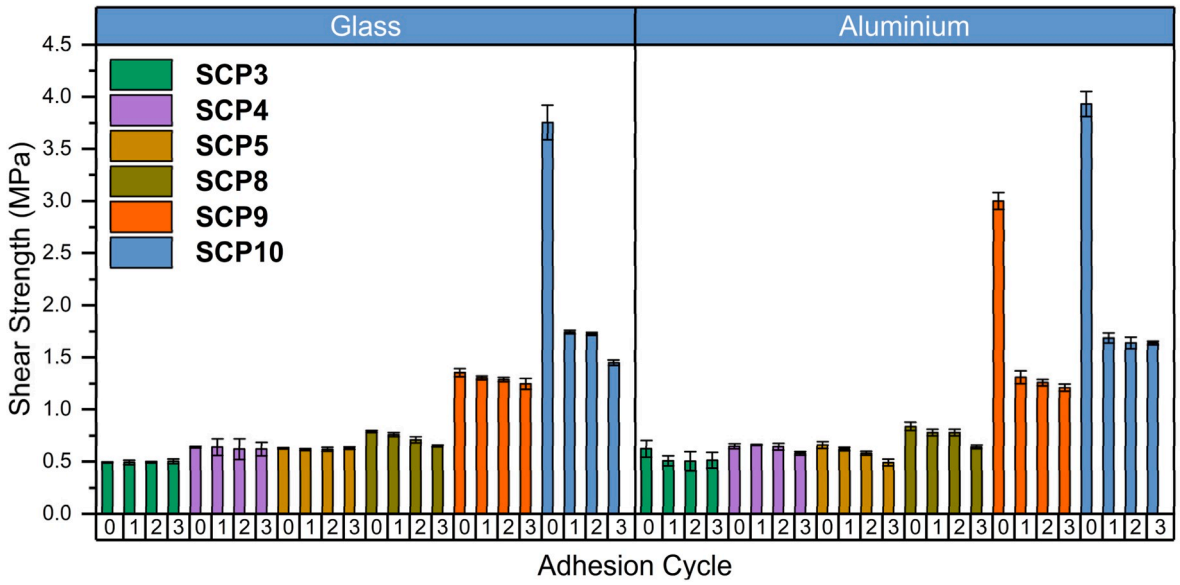

Fig. 4. Adhesive shear strength of **SCP3**-**SCP5** and **SCP8**-**SCP10** over three re-adhesion cycles on glass and aluminium substrates. The error shown is the standard deviation between the three repeats of each sample.

Table 5
The healed tensile values and healing efficiencies for **SCP3**-**SCP5** and **SCP8**-**SCP10**. The error shown is the standard deviation between the three repeats of each sample.

SCP	*meta (6)/para (7)*	mol% of 6/7	UTS (MPa)	Strain at break (ε)	Young's Modulus (MPa)	Modulus of Toughness (MJ m^{-3})
SCP3	**6**	**7.5**	0.06 ± 0.00	2.76 ± 0.00	0.28 ± 0.00	0.18 ± 0.00
			86 %	**48 %**	**140 %**	**69 %**
SCP4	**6**	**10.0**	0.08 ± 0.01	2.03 ± 0.01	0.38 ± 0.1	0.14 ± 0.03
			67 %	**82 %**	**64 %**	**78 %**
SCP5	**6**	**12.5**	0.11 ± 0.01	0.58 ± 0.1	0.64 ± 0.05	0.05 ± 0.01
			151 %	**36 %**	**168 %**	**66 %**
SCP8	**7**	**7.5**	0.05 ± 0.00	4.99 ± 0.9	0.30 ± 0.05	0.17 ± 0.02
			83 %	**41 %**	**88 %**	**53 %**
SCP9	**7**	**10.0**	0.25 ± 0.00	3.95 ± 0.4	0.62 ± 0.02	0.82 ± 0.1
			86 %	**61 %**	**91 %**	**58 %**
SCP10	**7**	**12.5**	0.52 ± 0.2	2.84 ± 0.2	1.11 ± 0.02	1.18 ± 0.1
			106 %	**60 %**	**82 %**	**59 %**

isomerisation within the pendant units of the polymer can affect the physical and mechanical properties of comb copolymers.

CRediT authorship contribution statement

Matthew Hyder: Writing – original draft, Visualization, Validation, Investigation, Formal analysis, Conceptualization. **Claudia Duval:** Writing – original draft, Visualization, Validation, Investigation, Formal analysis. **Lochlan J. McGregor:** Writing – original draft, Visualization, Validation, Investigation, Formal analysis. **Alarqam Z. Tareq:** Writing – original draft, Validation, Investigation, Formal analysis. **Adam D. O'Donnell:** Writing – review & editing, Investigation, Formal analysis. **Ann M. Chippindale:** Writing – review & editing, Formal analysis. **Josephine L. Harries:** Writing – review & editing, Supervision. **Wayne Hayes:** Writing – review & editing, Supervision, Resources, Project administration, Conceptualization.

Declaration of competing interest

The authors declare that they have no known competing financial interests or personal relationships that could have appeared to influence the work reported in this paper.

Acknowledgements

The authors would like to acknowledge the financial support from the University of Reading and Domino Printing Sciences Ltd (PhD studentship for M.H.) and from HCED Iraq (PhD studentship for A.Z.T.). In addition, the University of Reading (EPSRC – Doctoral Training Grant) is acknowledged for providing access to instrumentation in the Chemical Analysis Facility and the Centre for Advanced Microscopy. We thank Mr Nick Spencer (Chemical Analysis Facility (CAF), University of Reading) for collecting the single-crystal X-ray data.

Appendix A. Supplementary data

Supplementary data to this article can be found online at https://doi.org/10.1016/j.polymer.2025.128993.

Data availability

Data will be made available on request.

References

[1] J. Fox, J.J. Wie, B.W. Greenland, S. Burattini, W. Hayes, H.M. Colquhoun, M. E. Mackay, S.J. Rowan, High-strength, healable, supramolecular polymer nanocomposites, J. Am. Chem. Soc. 134 (2012) 5362–5368, https://doi.org/10.1021/ja300050x.

[2] A.D. O'Donnell, S. Salimi, L.R. Hart, T.S. Babra, B.W. Greenland, W. Hayes, Applications of supramolecular polymer networks, React. Funct. Polym. 172 (2022) 105209, https://doi.org/10.1016/j.reactfunctpolym.2022.105209.
[3] A. Feula, X. Tang, I. Giannakopoulos, A.M. Chippindale, I.W. Hamley, F. Greco, C. Paul Buckley, C.R. Siviour, W. Hayes, An adhesive elastomeric supramolecular polyurethane healable at body temperature, Chem. Sci. 7 (2016) 4291–4300, https://doi.org/10.1039/C5SC04864H.
[4] Z. Shen, Y. Jiang, T. Wang, M. Liu, Symmetry breaking in the supramolecular gels of an achiral gelator exclusively driven by π—π stacking, J. Am. Chem. Soc. 137 (2015) 16109–16115, https://doi.org/10.1021/jacs.5b10496.
[5] X. Li, Y. Wang, F. Li, X. Zhang, Fluorescent carbazole-containing dyes: synthesis and supramolecular assembly by self-complementary donor-acceptor π-stacking and dipolar interactions, Dyes Pigm 182 (2020) 108474, https://doi.org/10.1016/j.dyepig.2020.108474.
[6] S. Burattini, H.M. Colquhoun, J.D. Fox, D. Friedmann, B.W. Greenland, P.J. F. Harris, W. Hayes, M.E. Mackay, S.J. Rowan, A self-repairing, supramolecular polymer system: healability as a consequence of donor–acceptor π–π stacking interactions, Chem. Comm. 44 (2009) 6717–6719, https://doi.org/10.1039/b910648k.
[7] B.J. Holliday, C.A. Mirkin, Strategies for the construction of supramolecular compounds through coordination chemistry, Angew. Chem. Int. Ed. 40 (2001) 2022–2043, https://doi.org/10.1002/1521-3773(20010601)40:11<2022::AID-ANIE2022>3.0.CO;2-D.
[8] J.R. Kumpfer, J.J. Wie, J.P. Swanson, F.L. Beyer, M.E. Mackay, S.J. Rowan, Influence of metal ion and polymer core on the melt rheology of metallosupramolecular films, Macromolecules 45 (2012) 473–480, https://doi.org/10.1021/ma201659d.
[9] A. Harada, Y. Takashima, M. Nakahata, Supramolecular polymeric materials via cyclodextrin–guest interactions, Acc. Chem. Res. 47 (2014) 2128–2140, https://doi.org/10.1021/ar500109h.
[10] X.J. Loh, Supramolecular host–guest polymeric materials for biomedical applications, Mater. Horiz. 1 (2014) 185–195, https://doi.org/10.1039/C3MH00057E.
[11] R.P. Sijbesma, F.H. Beijer, L. Brunsveld, B.J.B. Folmer, J.H.K.K. Hirschberg, R.F. M. Lange, J.K.L. Lowe, E.W. Meijer, Reversible polymers formed from self-complementary monomers using quadruple hydrogen bonding, Science 278 (1997) 1601–1604, https://doi.org/10.1126/science.278.5343.1601.
[12] B. Isare, G. Pembouong, F. Boué, L. Bouteiller, Conformational control of hydrogen-bonded aromatic bis-ureas, Langmuir 28 (2012) 7535–7541, https://doi.org/10.1021/la300887p.
[13] B.C. Baker, I.M. German, A.M. Chippindale, C.E.A. McEwan, G.C. Stevens, H. M. Colquhoun, W. Hayes, Nitroarylurea-terminated supramolecular polymers that exhibit facile thermal repair and aqueous swelling-induced sealing of defects, Polymer 140 (2018) 1–9, https://doi.org/10.1016/j.polymer.2018.02.029.
[14] D.M. Wood, B.W. Greenland, A.L. Acton, F. Rodríguez-Llansola, C.A. Murray, C. J. Cardin, J.F. Miravet, B. Escuder, I.W. Hamley, W. Hayes, pH-Tunable hydrogelators for water purification: structural optimisation and evaluation, Chem. Eur J. 18 (2012) 2692–2699, https://doi.org/10.1002/chem.201102137.
[15] M. Burnworth, L. Tang, J.R. Kumpfer, A.J. Duncan, F.L. Beyer, G.L. Fiore, S. J. Rowan, C. Weder, Optically healable supramolecular polymers, Nature 472 (2011) 334–337, https://doi.org/10.1038/nature09963.
[16] R. Suriano, L. Brambilla, M. Tommasini, S. Turri, A deep insight into the intrinsic healing mechanism in ureido-pyrimidinone copolymers, Polym. Adv. Technol. 29 (2018) 2899–2908, https://doi.org/10.1002/pat.4409.
[17] J. Li, S. Luo, F. Li, S. Dong, Supramolecular polymeric pressure-sensitive adhesive that can be directly operated at low temperatures, ACS Appl. Mater. Interfaces 14 (2022) 27476–27483, https://doi.org/10.1021/acsami.2c05951.
[18] X. Callies, O. Herscher, C. Fonteneau, A. Robert, S. Pensec, L. Bouteiller, G. Ducouret, C. Creton, Combined effect of chain extension and supramolecular interactions on rheological and adhesive properties of acrylic pressure-sensitive adhesives, ACS Appl. Mater. Interfaces 8 (2016) 33307–33315, https://doi.org/10.1021/acsami.6b11045.
[19] W.H. Binder, L. Petraru, T. Roth, P.W. Groh, V. Pálfi, S. Keki, B. Ivan, Magnetic and temperature-sensitive release gels from supramolecular polymers, Adv. Funct. Mater. 17 (2007) 1317–1326, https://doi.org/10.1002/adfm.200601084.
[20] C. Kim, H. Ejima, N. Yoshie, Polymers with autonomous self-healing ability and remarkable reprocessability under ambient humidity conditions, J. Mater. Chem. A. Mater. 6 (2018) 19643–19652, https://doi.org/10.1039/C8TA04769C.
[21] M. Nakahata, Y. Takashima, H. Yamaguchi, A. Harada, Redox-responsive self-healing materials formed from host–guest polymers, Nat. Commun. 2 (2011) 511, https://doi.org/10.1038/ncomms1521.
[22] S. Cheng, M. Zhang, N. Dixit, R.B. Moore, T.E. Long, Nucleobase self-assembly in supramolecular adhesives, Macromolecules 45 (2012) 805–812, https://doi.org/10.1021/ma202122r.
[23] L.R. Hart, A.B.R. Touré, R. Owen, N.R.E. Putri, R.J.M. Hague, M.R. Alexander, F.R. A.J. Rose, Z. Zhou, D.J. Irvine, L. Ruiz-Cantu, L. Turyanska, Y. He, W. Hayes, R. D. Wildman, Screening of modular supramolecular star polymers for 3D printing of biomedical devices, Mater. Today Commun. 45 (2025) 112206, https://doi.org/10.1016/j.mtcomm.2025.112206.
[24] A.D. O'Donnell, A.G. Gavriel, W. Christie, A.M. Chippindale, I.M. German, W. Hayes, Conformational control of bis-urea self-assembled supramolecular pH switchable low-molecular-weight hydrogelators, ARKIVOC (Gainesville, FL, U. S.) 6 (2021) 222–241, https://doi.org/10.24820/ark.5550190.p011.581.
[25] S. Salimi, T.S. Babra, G.S. Dines, S.W. Baskerville, W. Hayes, B.W. Greenland, Composite polyurethane adhesives that debond-on-demand by hysteresis heating in an oscillating magnetic field, Eur. Polym. J. 121 (2019) 109264, https://doi.org/10.1016/j.eurpolymj.2019.109264.
[26] S. Chen, Z. Geng, X. Zheng, J. Xu, W.H. Binder, J. Zhu, Engineering the morphology of hydrogen-bonded comb-shaped supramolecular polymers: from solution self-assembly to confined assembly, Polym. Chem. 11 (2020) 4022–4028, https://doi.org/10.1039/D0PY00570C.
[27] M. Liu, Z. Wang, P. Liu, Z. Wang, H. Yao, X. Yao, Supramolecular silicone coating capable of strong substrate bonding, readily damage healing, and easy oil sliding, Sci. Adv. 5 (2019) eaaw5643, https://doi.org/10.1126/sciadv.aaw5643.
[28] J.H.K.K. Hirschberg, F.H. Beijer, H.A. van Aert, P.C.M.M. Magusin, R.P. Sijbesma, E.W. Meijer, Supramolecular polymers from Linear telechelic siloxanes with quadruple-hydrogen-bonded units, Macromolecules 32 (1999) 2696–2705, https://doi.org/10.1021/ma981950w.
[29] B.W. Greenland, M.B. Bird, S. Burattini, R. Cramer, R.K. O'Reilly, J.P. Patterson, W. Hayes, C.J. Cardin, H.M. Colquhoun, Mutual binding of polymer end-groups by complementary π–π-stacking: a molecular "Roman Handshake", Chem. Commun. 49 (2013) 454–456, https://doi.org/10.1039/C2CC35965K.
[30] Y. Chen, Z. Guan, Self-healing thermoplastic elastomer brush copolymers having a glassy polymethylmethacrylate backbone and rubbery polyacrylate-amide brushes, Polymer 69 (2015) 249–254, https://doi.org/10.1016/j.polymer.2015.03.023.
[31] K. Zhang, M. Aiba, G.B. Fahs, A.G. Hudson, W.D. Chiang, R.B. Moore, M. Ueda, T. E. Long, Nucleobase-functionalized acrylic ABA triblock copolymers and supramolecular blends, Polym. Chem. 6 (2015) 2434–2444, https://doi.org/10.1039/C4PY01798F.
[32] M. Chen, D.L. Inglefield, K. Zhang, A.G. Hudson, S.J. Talley, R.B. Moore, T.E. Long, Synthesis of urea-containing ABA triblock copolymers: influence of pendant hydrogen bonding on morphology and thermomechanical properties, J. Polym. Sci. A. Polym. Chem. 56 (2018) 1844–1852, https://doi.org/10.1002/pola.29066.
[33] B.D. Mather, M.B. Baker, F.L. Beyer, M.A.G. Berg, M.D. Green, T.E. Long, Supramolecular triblock copolymers containing complementary nucleobase molecular recognition, Macromolecules 40 (2007) 6834–6845, https://doi.org/10.1021/ma070865y.
[34] C.L. Elkins, T. Park, M.G. McKee, T.E. Long, Synthesis and characterization of poly (2-ethylhexyl methacrylate) copolymers containing pendant, self-complementary multiple-hydrogen-bonding sites, J. Polym. Sci. A. Polym. Chem. 43 (2005) 4618–4631, https://doi.org/10.1002/pola.20961.
[35] F. Rodríguez-Llansola, B. Escuder, J.F. Miravet, D. Hermida-Merino, IanW. Hamley, C.J. Cardin, W. Hayes, Selective and highly efficient dye scavenging by a pH-responsive molecular hydrogelator, Chem. Comm. 46 (2010) 7960, https://doi.org/10.1039/c0cc02338h.
[36] B.C. Baker, A.L. Acton, G.C. Stevens, W. Hayes, Bis Amide-Aromatic-ureas—highly effective hydro- and organogelator systems, Tetrahedron 70 (2014) 8303–8311, https://doi.org/10.1016/j.tet.2014.09.017.
[37] C. van Sloun, O. Peters, M. Tabatabai, H. Ritter, Molecular Recognition: influence of *Para* -Versus- *Meta* -Substituted Phenyl Moieties on the Swelling Degree of Macroscopic Polymeric Gels in Aqueous Cyclodextrin Solutions, Macromol. Rapid Commun. 34 (2013) 1560–1562, https://doi.org/10.1002/marc.201300428.
[38] K. Shibata, M. Hayashi, Y. Inai, Experimental and theoretical investigation of intrinsic pyridine isomer effects on physical property tuning of metallo supramolecular polymers bearing multiple pyridine ligands, ACS Appl. Polym. Mater. 2 (2020) 2327–2337, https://doi.org/10.1021/acsapm.0c00284.
[39] F. Xu, B.L. Feringa, Photoresponsive supramolecular polymers: from light-controlled small molecules to smart materials, Adv. Mater. 35 (2023) 2204413, https://doi.org/10.1002/adma.202204413.
[40] S. Tamesue, Y. Takashima, H. Yamaguchi, S. Shinkai, A. Harada, Photoswitchable supramolecular hydrogels formed by cyclodextrins and azobenzene polymers, Angew. Chem. Int. Ed. 49 (2010) 7461–7464, https://doi.org/10.1002/anie.201003567.
[41] Y. Zhao, F.J. Stoddart, Azobenzene-based light-responsive hydrogel system, Langmuir 25 (2009) 8442–8446, https://doi.org/10.1021/la804316u.
[42] N. Bajaj, L.R. Hart, B.W. Greenland, W. Hayes, Urea organogelators – synthesis and properties, Macromol. Symp. 329 (2013) 118–124, https://doi.org/10.1002/masy.201200103.
[43] B.C. Baker, I.M. German, G.C. Stevens, H.M. Colquhoun, W. Hayes, Synthesis and analysis of a healable, poly(propylene glycol)- based supramolecular network, Prog. Org. Coat. 127 (2019) 260–265, https://doi.org/10.1016/j.porgcoat.2018.11.029.
[44] B.C. Baker, I.M. German, A.M. Chippindale, C.E.A. McEwan, G.C. Stevens, H. M. Colquhoun, W. Hayes, Nitroarylurea-terminated supramolecular polymers that exhibit, facile thermal repair and aqueous swelling-induced sealing of defects, Polymer 140 (2018) 1–9, https://doi.org/10.1016/j.polymer.2018.02.029.
[45] M. Hyder, A.D. O'Donnell, A.M. Chippindale, I.M. German, J.L. Harries, O. Shebanova, I.W. Hamley, W. Hayes, Tailoring viscoelastic properties of dynamic supramolecular poly(butadiene)-based elastomers, Mater. Today Chem. 26 (2022) 101008, https://doi.org/10.1016/j.mtchem.2022.101008.
[46] Z. Shi, M. Hyder, A.Z. Tareq, A.M. Chippindale, J.A. Cooper, J.L. Harries, W. Hayes, Adhesive and healable supramolecular comb-polymers, React. Funct. Polym. 202 (2024) 105994, https://doi.org/10.1016/j.reactfunctpolym.2024.105994.
[47] S. Burattini, B.W. Greenland, D. Hermida Merino, W. Weng, J. Seppala, H. M. Colquhoun, W. Hayes, M.E. Mackay, I.W. Hamley, S.J. Rowan, A healable supramolecular polymer blend based on aromatic π-π stacking and hydrogen-bonding interaction, J. Am. Chem. Soc. 132 (2010) 12051–12058, https://doi.org/10.1021/ja104446r.
[48] A.Z. Tareq, M. Hyder, D.H. Merino, A.M. Chippindale, A. Kaur, J.A. Cooper, W. Hayes, Thermally and mechanically robust self-healing supramolecular

polyurethanes featuring aliphatic amide end caps, Polymer 302 (2024) 127052, https://doi.org/10.1016/j.polymer.2024.127052.
[49] L.R. Hart, N.A. Nguyen, J.L. Harris, M.E. Mackay, H.M. Colquhoun, W. Hayes, Perylene as an electron-rich moiety in healable, complementary π-π stacked, Polymer 69 (2015) 293–300, https://doi.org/10.1016/j.polymer.2015.03.028, supramolecular polymer systems.
[50] K. Yamauchi, J.R. Lizotte, T.E. Long, Thermoreversible poly(alkyl acrylates) consisting of self-complementary multiple hydrogen bonding, Macromolecules 36 (2003) 1083–1088, https://doi.org/10.1021/ma0212801.
[51] K. Kojio, S. Kugumiya, Y. Uchiba, Y. Nishino, M. Furukawa, The microphase-separated structure of polyurethane bulk and thin films, Polym. J. 41 (2009) 118–124, https://doi.org/10.1295/polymj.PJ2008186.
[52] E. Nagao, J.A. Dvorak, Phase imaging by atomic force microscopy: analysis of living homoiothermic vertebrate cells, Biophys. J. 76 (1999) 3289–3297, https://doi.org/10.1016/S0006-3495(99)77481-3.
[53] J.T. Garrett, C.A. Siedlecki, J. Runt, Microdomain morphology of poly(urethane urea) multiblock copolymers, Macromolecules 34 (2001) 7066–7070, https://doi.org/10.1021/ma0102114.
[54] A.Z. Tareq, M. Hyder, D.H. Merino, S.D. Mohan, J.A. Cooper, W. Hayes, Design and synthesis of aliphatic supramolecular polymers featuring amide, urethane, and urea hydrogen bonding units, Eur. Polym. J. 228 (2025) 113782, https://doi.org/10.1016/j.eurpolymj.2025.113782.
[55] O.J.G.M. Goor, H.M. Keizer, A.L. Bruinen, M.G.J. Schmitz, R.M. Versteegen, H. M. Janssen, R.M.A. Heeren, P.Y.W. Dankers, Efficient functionalization of additives at supramolecular material surfaces, Adv. Mater. 29 (2017) 1604652, https://doi.org/10.1002/adma.201604652.
[56] F. Yeh, B.S. Hsiao, B.B. Sauer, S. Michel, H.W. Siesler, In-Situ studies of structure development during deformation of a segmented poly(urethane−urea) elastomer, Macromolecules 36 (2003) 1940–1954, https://doi.org/10.1021/ma0214456.
[57] S. Han, G. Mellot, S. Pansec, J. Rieger, F. Stoffelbach, E. Nicole, O. Colombani, J. Jestin, L. Bouteiller, Crucial role of the spacer in tuning the length of self-assembled nanorods, Macromolecules 53 (2020) 427–433, https://doi.org/10.1021/acs.macromol.9b01928.
[58] E. Ressouche, S. Pensec, B. Isare, J. Jestin, L. Bouteiller, Two-component self-assemblies : investigation of a synergy between bisurea stickers, Langmuir 32 (2016) 11664–11671, https://doi.org/10.1021/acs.langmuir.6b03325.
[59] X. Callies, E. Ressouche, C. Fonteneau, G. Ducouret, S. Pensec, L. Bouteiller, C. Creton, Effect of the strength of stickers on rheology and adhesion of supramolecular centre-functionalized polyisobutenes, Langmuir 42 (2018) 12625–12634, https://doi.org/10.1021/acs.langmuir.8b02533.
[60] D.W.R. Balkenende, C.A. Monnier, G.L. Fiore, C. Weder, Optically responsive supramolecular polymer glasses, Nat. Commun. 7 (2016) 10995, https://doi.org/10.1038/ncomms10995.
[61] D. Döher, J. Kang, C.B. Cooper, J.B.-H. Tok, H. Rupp, W.H. Binder, Z. Bao, Tuning the self-healing response of poly(dimethylsiloxane)-based elastomers, ACS Appl. Polym. Mater. 2 (2020) 4127–4139, https://doi.org/10.1021/acsapm.0c00755.
[62] L.N. Neumann, E. Oveisi, A. Petzold, R.W. Style, T. Thurn-Albrecht, C. Weder, S. Schrettl, Dynamics and healing behavior of metallosupramolecular polymers, Sci. Adv. 7 (2021), https://doi.org/10.1126/sciadv.abe4154 eabe4154.